Elastic Moduli Determination of MgO Using Ultrasonic Interferometry

초음파 간섭법을 이용한 MgO 단결정의 체적탄성률 측정

Young-Ho Kim (김영호)

Department of Earth and Environmental Science, College of Natural Sciences
Gyeongsang National University, Jinju 660-701, Korea
(경상대학교 자연과학대학 지구환경과학과, E-mail: yhkim@nongae.gsnu.ac.kr)

ABSTRACT : Using the ultrasonic interferometry on the single crystal MgO-periclase, adiabatic bulk moduli were determined to be 163.2 GPa and 162.6 GPa from (100) and (110) lattice plane measurements, respectively. Density was measured on polycrystalline MgO by the X-ray diffraction technique. Results from this study were compared with the previously reported values. Further, the present results were converted to the isothermal bulk moduli and, then compared with the published data available including the energy dispersive X-ray diffraction result which was performed on the same single crystal MgO. The principle and techniques of ultrasonic interferometry were introduced too.

Keywords : ultrasonic interferometry, bulk moduli, adiabatic, isothermal

요약 : MgO-페리클레이즈 단결정의 체적탄성률을 초음파 간섭법을 이용하여 측정하였는데 (100) 면과 (110)면에 대한 초음파속도 측정치로부터 계산된 값은 각각 163.2 GPa 와 162.6 GPa 이다. 이 계산에 이용된 MgO의 밀도는 동일 단결정을 분쇄하여 얻은 분말 시료를 X-선 회절법을 이용하여 결정하였다. 이러한 실험 결과를 기존의 값과 비교하였고, 이를 등온 체적탄성률로 변환하여 동일한 시료를 이용하여 시행된 에너지 분산 X-선 회절 실험 결과를 포함하는 실험 결과치와 비교하였다. 초음파 간섭법의 원리와 방법도 소개되었다.

주요어 : 초음파 간섭법, 체적탄성률, 단열, 등온

Introduction

MgO-periclase as well as MgSiO$_3$-perovskite is the major constituent in the lower mantle of the Earth (Brown and Mussett, 1993). In view of this importance, there has been a lot of studies performed in the various properties on MgO : thermodynamic properties (Anderson and Zou, 1989; Chopelas, 1990), thermochemistry (Saxena and Zhang, 1990), equation of state study by molecular dynamics (Kubicki, 1988) as well as by the ultrasonic method (Spetzler, 1970) and energy dispersive X-ray diffraction method (Manghnani et al., 1987), electrical properties (Wood and Nell, 1991), and elastic properties (Zouboulis and Grimsditch, 1991).

Among these studies, employing the cubic anvil apparatus interfaced with synchrotron radiation and energy dispersive X-ray diffraction (EDXRD) technique in the hydrostatic conditions, MgO-periclase bulk modulus of 158.06 GPa was obtained using the Birch-Murghnan equation of state with the assumed K_0' of 4.15 (Manghnani et al., 1987). MgO single crystal used for the present study is the same as the EDXRD compression experiment employed. Objectives of this study are the followings: (1) introduce the principles and techniques of the ultrasonic interferometry (2) measure the sound wave velocity in a particular crystal direction of MgO using the ultrasonic interferometry, (3) calculate the density of MgO from measurement of unit cell volume of polycrystalline MgO sample by Debye-Scherrer method, (4) determine the elastic modulus of MgO from the measurement of sound velocity and density with some correction procedure, and (5) compare this result with the previously reported values as well as the EDXRD compression datum which was performed on the same single crystal.

Experimental Methods

Sample Preparations

Single crystal MgO : Single crystal MgO used in this study was provided by Mr. Edward Fisher at the Argonne National Laboratory in USA. This single crystal was grown along c-axis and then cut along each crystallographic axis, and polished on each crystal plane in the grounding system with various resins manually.

In order to check the orientation of (100) lattice plane, the prepared specimen was loaded in the two-circle goniometer configurated with Laue back-reflection camera. Laue spots were examined in the Greninger chart, and the center was turned out to be $2°$ off between the diffraction pattern of (100) plane and the direct beam of x-radiation spot. This center-off was adjusted using two-circle goniometer. After this adjustment, the position of the (100) crystal

plane was checked again to make it in right position.

The adjusted side of (100) plane was aligned parallel to the brass ring in order to make the opposite side parallel to the adjusted side by grinding. The brass ring mounted with sample was ground by the automatic grinding machine, and then polished by the appropriate diamond pastes manually. The thickness of the sample prepared such a way was measured to be 0.3849 inch. The (110) crystal plane was prepared using the same procedures described above, and thickness was 0.2405 inch.

Polycrystalline MgO : For X-ray density measurement, polycrystalline MgO was prepared from single crystal pieces during the cutting of the bulky crystal. These pieces were ground in the agate mortar thoroughly, then crystalline grain size was checked in the XRD camera.

Experimental Techniques

Ultrasonic interferrometry : A schematic ultrasonic interferrometry diagram is shown in Fig. 1. A frequency synthesizer is used to provide a carrier frequency of 20 MHz. Output of the synthesizer is brought in to an pulsed oscillator, which is operated as a gated amplifier. These pulses control the on time of the 20-MHz RF bursts. An isolation network consisting of four diodes and an attenuator is used to protect the pulse generator from back reflections. The impedance between the isolation network and quartz transducer is matched when necessary with an air-coupled transformer. The return signals from the transducer are applied without amplification to the top trace of the oscilloscope. The input of the tunable amplifier is protected by the another isolation network. The main sweep of the oscilloscope is triggered from dual pulse generator. Each pulse from generator also triggers a fast rise time pulse generator which provides the input signal to an time-interval counter. The time between the two RF pulses is thus read on the time-interval counter and is equal
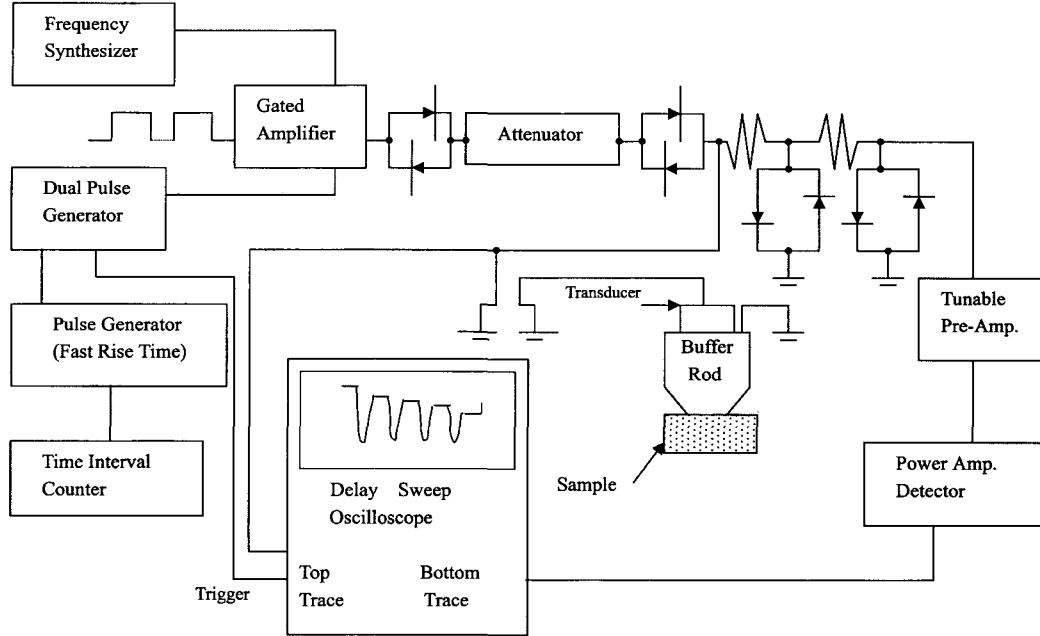
Fig. 1. Schematic diagram of the ultrasonic interferometry system.

to twice the travel time through the sample.

In order to determine the phase shift at the buffer-rod sample interface and at the free end of the sample, following facts should be considered : The acoustic impedance of a substance is defined as the product of velocity times density. Consider plane waves normally incident to a plane boundary that separates two media, 1 and 2, having acoustic impedances R_1 and R_2, respectively. Let R_1 be smaller than R_2 ; a sound wave traveling from medium 1 into medium 2 will be reflected without any change in phase of stress. On the other hand, if the wave is incident from medium 2, the stress wave reflected into medium 2 will show a phase shift of π radians.

The buffer-rod sample system is illustrated in Fig. 2. Let the impedance of the buffer rod and the sample be R_1 and R_2, respectively. When the buffer rod impedance is less than the impedance of the sample, every reflection within the sample causes a phase shift of π. In the case where the buffer-rod impedance is higher,

a phase shift of π within the sample is only realized at the free end. If the case $R_1 < R_2$, the total phase shift within the sample may be written for the nth echo that is received from the free end, $\Phi_n = [1 + 2n(2l - m\lambda/\lambda)]\pi$ where l is the sample length, λ is the acoustic wavelength in the sample, and m is an integer denoting the number of whole wavelengths within $2l$. Maximum or minimum interference between the echo trains of the two applied pulses occurs only if $(2l - m\lambda)/\lambda$ is zero or half-integer. Let $(2l - m\lambda)/\lambda$ equal to zero, which implies that there is an integral m multiple of the wavelength in $2l$. All echoes are phase shifted by an equal amount, and this addition results in a maximum amplitude; i.e., the velocity can be written as $V = 2lf/m$ where f is the carrier frequency where a maximum occurs. When $(2l - m\lambda)/\lambda = 1/2$, $\Phi_n = (n + 1)\pi$, i.e., the phase shift between consecutive echoes alternates by π, and a minimum in amplitude is realized for an applied pulse spacing equal to one round-trip time in the sample. In Fig. 2,
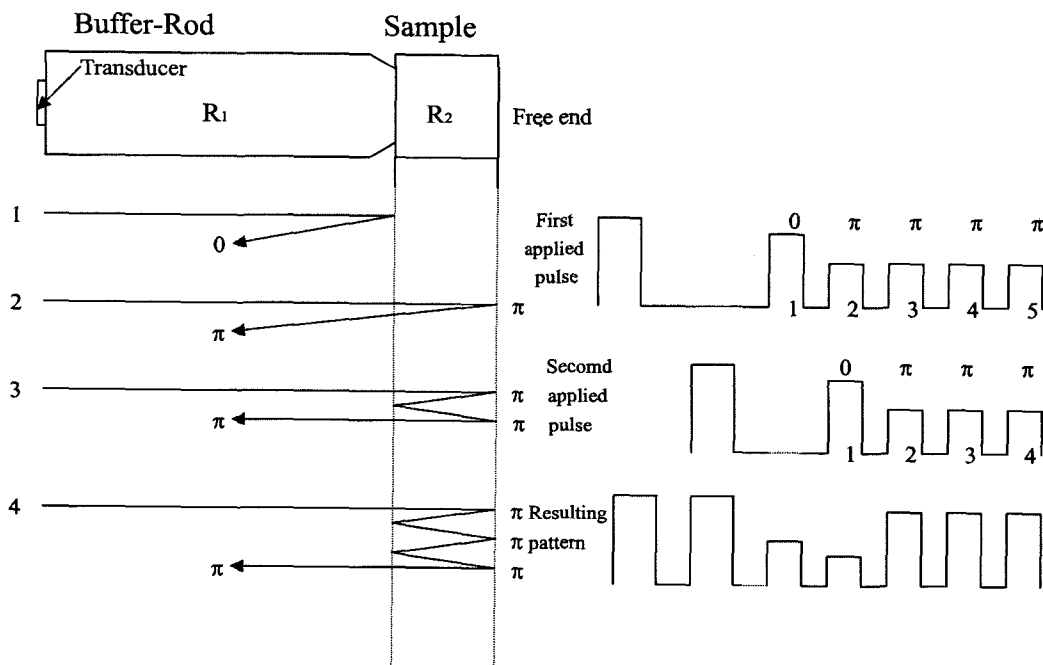
Fig. 2. Schematic diagram of the buffer-rod sample system and phase shifts of stress waves in case of $R_1 < R_2$.

the phase shifts of wave are shown in the case of $R_1 < R_2$.

For the case where $R_1 > R_2$, the phase shift in the sample can be written as $\Phi_n = n \pi [(l + 2(2l-m \lambda / \lambda)]$. In this case of periclase, however, since impedance of MgO is larger than that of buffer-rod, explanation where $R_1 > R_2$ is omitted and representation of the phase shifts of waves is not given in Fig. 2 either.

The sample with (100) crystal plane was fixed on the buffer rod using the paste of Non-ag stopcock grease and phenyl salicylate for longitudinal and transverse velocity measurements, respectively. The (110) crystal plane was prepared by the same method for sound velocity measurement. When you control the transducer, you can generate either longitudinal wave or transverse wave. In one mode of waves, when you can increase the number of whole wave-lengths (i.e., *m* in the appendix & Table 2) within the sample, you can get the frequency values corresponding to the each number of

wavelength. Then, you can calculate the average frequency on each run (see appendix & Table 2 for detail).

X-ray density measurement : Unit cell volume of MgO powder was determined by Debye-Scherrer XRD technique. NaCl powder was mixed with polycrystalline MgO at the ratio of 1 : 1 in volume. Mixture of powders was inserted in the capillary tube, and positioned at the center of the XRD camera as closely as possible by hand manipulation. For more precise measurement, NaCl was mixed and its diffraction lines were used to correct the geometry of the Debye-Scherrer camera.

Results and Discussion

X-ray density measurement is crucial for the determination of the elastic constant in this procedure. Lattice parameter was determined from four diffraction lines of (111), (200), (220) and

(222) of MgO polycrystalline sample. Using these values, lattice parameter of MgO was determined to be 4.215(1) Å. This is fairly good agreement with ASTM one (4-0829) of 4.213 Å. From this unit cell volume, x-ray density of MgO was calculated to be 3.575 gr/cm^3 (c.f., 3.581 gr/cm^3 of 4-0829 in ASTM).

The bulk modulus of MgO single crystal were calculated using the relation $K_s = (C_{11} + 2 \times C_{12})/3$ for (100) and (110) planes as follows; $K_{s, (100)} = 163.2$ GPa and $K_{s, (110)} = 162.6$ GPa. For determination of this value in (100) direction, correction was compulsory because of 2° off at center. Therefore, 2° off correction and the bulk modulus calculation methods were given in appendix.

Comparison of this result with the previously reported data were given in Table 1. Densities of the previous studies are slightly higher than the present one. This might be caused by the synthetic processes of the MgO single crystal as well as the systematic deviations in the XRD measurements of densities or different density measuring methods. However, Jackson and Niesler (1982) and Yoneda (1990) reported the very close values to the present result.

The present value indicates the adiabatic bulk modulus. When you convert this to the isothermal bulk modulus, you can compare this value with the compression results at high pressure on either single crystal or polycrystalline samples. The relationship between K_S and K_T is the following : $K_S = K_T(1 + \alpha \gamma T)$, where α is

the thermal expansion coefficient, γ is the Gruneisen parameter, and T is the temperature in Kelvin. With the reported values of both thermal expansion coefficient, 31.2×10^{-6}/degree (Suzuki, 1975), and Gruneisen parameter of 1.54 (Anderson et al., 1965) for MgO, the isothermal bulk moduli of 160.9 GPa and 160.3 GPa from the present data were calculated to the (100) and (110) plane, respectively at ambient temperature. Drickamer et al., (1966) determined the bulk modulus of MgO using his own Drickamer press up to 30 GPa and reported the value of 178 GPa under the assumption of K_0' at 4.0 fitting his compression date to the Murghnan equation of state. After this work, Mao and Bell (1979) reported the bulk modulus to be 159 GPa with K_0' of 4.7 from the polycrystalline MgO powder in the diamond anvil cell. Using single crystal of MgO in the cubic-anvil apparatus interfaced with synchrotron radiation in the EDXRD mode, bulk modulus of 158.06 GPa was obtained by the fitting to the Birch-Murghnan equation of state under the assumption of K_0' to be 4.15 (Manghnani et al., 1987). From the latter two results, Drickamer's value turned out to be rather high and this result might be caused from both the apparatus used in different style and the method which determined the high pressure values. Comparing Manghnani et al.,'s with the present result which the samples from same single crystal were used, compression result appears to be lower than that from the ultrasonic interfer-

Table 1. Comparison of the bulk modulus of MgO

Density \ C	C_{11}	C_{44}	C_{12}	K_S	References
3.581	297.4	156.2	95.6	162.8	Spetzler (1970)
3.584	294	155	93	160	Hearmon (1979)
3.584	296.8	155.8	95.3	162.5	Jackson & and Niesler (1982)
3.584	297.8	155.8	95.1	162.7	Yoneda (1990)
3.575	297.5	156.2	95.5	162.6	This study, (110)

ometrical determination. This difference might be caused from systematic errors dependent on the different apparatus environment used for measurement. However, bulk moduli determined from both elastic measurement and X-ray diffraction techniques show the constant trend within their own experimental errors.

Geophysically, MgO in the lower mantle plays important role in whether would be adapted either olivine series or pyroxene series of the Earth mantle model. As a simple cubic crystal structure, elastic properties of MgO have some implications for the propagations of the longitudinal and transverse waves in the lower mantle where the perovskite structured silicate in the orthorhombic crystal system is dominated.

The present study can be summarized as follows : Using ultrasonic interferometry on the single crystal MgO, bulk moduli were determined to be 163.2 GPa and 162.6 GPa from (100) and (110) lattice plane measurements, respectively. Density of MgO was determined on MgO powder from same single crystal using XRD technique. Adiabatic bulk moduli at the present experiment were converted to the isothermal ones, and both values were compared with the reported data, respectively.

Acknowledgments

References

Anderson, G. D., Doran, G. D. and Fahrenbruch, A. L. (1965) Stanford Reserach Institute, Menlo Park, Calif., AFWL-TR-65-147 and AFWL-TR-65-43

Anderson, O. L. and Zou, K. (1989) Formulation of the thermodynamic functions for mantle minerals: MgO as an example, Phys. Chem. Minerals, 16(7), 642-648

Brown, G. C. and Mussett, A. E. (1993) The inaccessible Earth, An integrated view to its structure and composition, Chapman & Hall, 276

Chopelas, A. (1990) Thermal expansion, heat capacitym and entropy of MgO at mantle pressures, Phys. Chem. Minerals, 17(2), 142-148

Drickamer, H. G., Lynch, R. W., Clendenen, R. L. and Perez-Albuerne, E. A. (1966) X-ray diffraction studies of the lattice parameters of solids under very high pressure, Solid State Physics, 19, 135-229

Hearmon, R. F. S. (1979) The elastic constants of crystals and other anisotropic materials, in Landolt-Bornstein Tables, III/11, edited by K. H. Hellwege and A. M. Hellewege, Springer-Verlag, 854

Jackson, I. and Niesler, H. (1982) The elasticity of periclase to 3 GPa and some geophysical implications, in High-Pressure Research in Geophysics, Advances in Earth and Planetary Sciences, 12, edited by S. Akimoto and M.H. Manghnani, Center for Academic Publications, Tokyo, 93-113

Kubicki, J. D. (1988) Periclase and MgSiO$_3$-perovskite equations of state using many- body molecular dynamics, Annul Report of the Director Geiphysical Laboratory, 1987-1988, 81-84

Manghnani, M. H., Ming, L. C., Shimomura, O., Susaki, J., Yagi, T., Akimoto, S., Ito, E. and Nakagiri, N. (1987) Hydrostatic compression of MgO and MgO-FeO to 6.2 GPa, X-ray measurements using Synchrotron Radiation, Eos, 68(16), 409

Mao, H. K. and Bell, P. M. (1979) Equation of state of MgO and ε-iron under static pressure conditions, J. Geophys. Res., 84, 4533-4536

Saxena, S. K. and Zhang, J. (1990) Thermochemical and pressure-volume-temperature systematics of data on solids, examples: tungsten and MgO, Phys. Chem. Minerals, 17(1), 45-51

Spetzler, H. (1970) Equation of state of polycrystalline and single-crystal MgO to 8 kilobar and 800 K, J. Geophys. Res., 75(11), 2073-

2087

Suzuki, I. (1975) Thermal expansion of periclase and olivine and their anharmonic properties, J. Phys. Earth, 23, 145-159

Wood, B. J. and Nell, J. (1991) High-temperature electrical conductivity of the lower mantle phase (Mg,Fe)O, Nature, 351, 309-311

Yoneda, A. (1990) Pressure derivatives of elastic constants of single crystal MgO and MgAl$_2$O$_4$, J. Phys. Earth, 38, 19-55

Zouboulis, E. S. and Grimsditch, M. (1991) Refractive index and elastic properties of MgO up to 1900 K, J. Geophys. Res., 96(B3), 4167-4170

Appendix

In order to correct the $2°$ center-off in Laue pattern, consider the Cartesian coordinate system, and directional cosines of $l = \cos\theta$, $m = \cos(90 + \theta) = -\sin\theta$ and $n = n$.
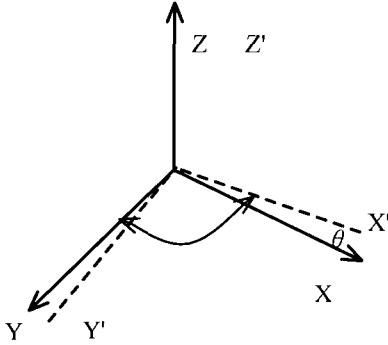
We can express the relation of the coordinates axis change as follows;

coordinate axis	X	Y	Z
X'	$\cos\theta * l$	$-\sin\theta * l$	0
Y'	$\sin\theta$	$\cos\theta$	0
Z'	0	0	1

(1)

The general equations of motion, in the absence of damping are

$$- \rho\frac{d^2u}{dt^2} = \frac{dX_x}{dx} + \frac{dX_y}{dy} + \frac{dX_z}{dz} \text{ with}$$

similar expressions for v and w.

This equation can be written in terms of u, v, w and directional cosine, by introducing new moduli Γ_{ij}, which are functions of the elastic constants C_{hk}, and of l, m, n.

$$\rho\frac{d^2u}{dt^2} = \Gamma_{11}\frac{d^2u}{ds^2} + \Gamma_{12}\frac{d^2v}{ds^2} + \Gamma_{13}\frac{d^2w}{ds^2}$$

with similar expressions for v and w, and where s $= lx + my + nz$.

Γ_{ij} can be written by Christoffel equation as follows :

$\Gamma_{11} = l^2C_{11} + m^2C_{66} + n^2C_{55} + 2mnC_{56} + 2nlC_{51} + 2lmC_{16}$

$\Gamma_{22} = l^2C_{66} + m^2C_{22} + n^2C_{44} + 2mnC_{24} + 2nlC_{46} + 2lmC_{26}$

$\Gamma_{33} = l^2C_{55} + m^2C_{44} + n^2C_{33} + 2mnC_{34} + 2nlC_{35} + 2lmC_{45}$

$\Gamma_{23} = l^2C_{56} + m^2C_{24} + n^2C_{34} + mn(C_{23}+C_{44}) + nl(C_{45}+C_{36}) + lm(C_{46}+C_{25})$

$\Gamma_{31} = l^2C_{15} + m^2C_{46} + n^2C_{35} + mn(C_{45}+C_{36}) + nl(C_{31}+C_{55}) + lm(C_{56}+C_{14})$

$\Gamma_{12} = l^2C_{15} + m^2C_{26} + n^2C_{45} + mn(C_{46}+C_{25}) + nl(C_{56}+C_{14}) + 2lm(C_{12}+C_{66})$

The solution of Christoffel equation can be written by

$$\begin{vmatrix} \Gamma_{11} - q & \Gamma_{12} & \Gamma_{13} \\ \Gamma_{12} & \Gamma_{22} - q & \Gamma_{23} \\ \Gamma_{13} & \Gamma_{23} & \Gamma_{33} - q \end{vmatrix} = 0 \quad (2)$$

where q is the stiffness factor.
From (1), we can rewrite (2) like

$$\begin{vmatrix} \Gamma_{11} - q & \Gamma_{12} & 0 \\ \Gamma_{12} & \Gamma_{22} - q & 0 \\ 0 & 0 & \Gamma_{33} - q \end{vmatrix} = 0 \quad (3)$$

where $\Gamma_{11} = C_{11} \cdot \cos^2\theta + C_{44} \cdot \sin^2\theta$, $\Gamma_{22} = C_{44} \cdot \cos^2\theta + C_{11} \cdot \sin^2\theta$, $\Gamma_{33} = C_{44}$ and

$$\Gamma_{12} = -\sin\theta \cdot \cos\theta \cdot (C_{12} + C_{44}) \quad (4)$$

Solving (3) with substituting (4) and then

inserting θ of $2°$, you have

$$q = C_{11} + C_{44} +/- [0.9952(C_{11} - C_{44})^2 + 0.0049(C_{12} + C_{44})^2]^{1/2} \tag{5}$$

From the relationship in (100) plane,

$$\rho V_L^2 = C_{11}, \quad \rho V_{T1}^2 = C_{44}, \quad \rho V_{T2}^2 = C_{44} \tag{6}$$

and, from the measurements of frequency for longitudinal wave (see Table 2),

$$V_L = 2\Delta f/m = 2 * 2.54 * 0.3849 * 0.4663(\text{MHz})$$
$$= 0.91175 * 10^6 \text{ cm/sec} \tag{7}$$
$$\rho V_L^2 = 2.972 * 10^{12} \text{ gr/cm} \cdot \text{sec}^2.$$

From the measurements of frequency for trans-

Table 2. Velocity measurement data by ultrasonic interferometry

Longitudinal transducer			Transverse transducer*		
Frequency, MHz	m	$\Delta f = f/m$	Frequency, MHz	m	$\Delta f = f/m$
29.855	64	0.4665	10.791	32	0.3372
30.322	65	0.4665	11.469	34	0.3373
30.781	66	0.4664	12.146	36	0.3374
31.268	67	0.4667	12.823	38	0.3374
31.716	68	0.4664	13.490	40	0.3373
32.165	69	0.4662	14.166	42	0.3373
32.652	70	0.4665	14.845	44	0.3373
33.116	71	0.4664	15.521	46	0.3374
33.600	72	0.4667	16.193	48	0.3374
34.051	73	0.4665	16.870	50	0.3374
34.508	74	0.4663	17.547	52	0.3374
34.985	75	0.4665	18.212	54	0.3374
35.446	76	0.4664	18.893	56	0.3373
35.917	77	0.4665	19.568	58	0.3374
36.377	78	0.4664	20.252	60	0.3375
36.826	79	0.4662	20.926	62	0.3375
37.301	80	0.4663	21.599	64	0.3375
37.767	81	0.4663	22.273	66	0.3375
38.236	82	0.4663	22.953	68	0.3375
38.689	83	0.4661	23.620	70	0.3374
39.175	84	0.4664	24.294	72	0.3374
39.629	85	0.4662	24.970	74	0.3374
40.086	86	0.4661	25.639	76	0.3374
40.569	87	0.4663	26.315	78	0.3374
41.008	88	0.4660	26.989	80	0.3374
41.477	89	0.4660	27.666	82	0.3374
41.962	90	0.4662	28.337	84	0.3373
42.400	91	0.4659	29.014	86	0.3374
42.885	92	0.4661	29.687	88	0.3374
43.354	93	0.4662	30.367	90	0.3374
43.807	94	0.4660	31.036	92	0.3373
44.292	95	0.4662			
44.745	96	0.4661			
45.216	97	0.4661			
45.69	98	0.4662			
46.151	99	0.4662			
46.625	100	0.4663			
47.072	101	0.4661			
Average		0.4663	Average		0.3374

*Due to the lengthy data points, even numbers were selected and shown in this table. At odd number of m (the number of whole wavelengths), each frequency was measured.

verse wave (Table 2),

$$V_T = 2 * 2.54 * 0.3849 * 0.3374 \text{ (MHz)}$$
$$= 0.65972 * 10^6 \text{ cm/sec} \qquad (8)$$
$$\rho V_T^2 = 1.5559 * 10^{12} \text{ gr/cm} \cdot \text{sec}^2$$

If, $\triangle \theta = 0°$, then $C_{11} = 2.972$,
$$C_{44} = 1.5559 \text{ in Mbar} \qquad (9)$$

However, (100) plane is $2°$ off and this discrepancy is as follows;

$$q = 2 \rho V_L^2 = 2.972 + 1.5558 + [0.9952$$
$$(C_{11} - C_{44})^2 + 0.0049 \ (C_{12} + C_{44})^2]^{1/2} \qquad (10)$$

From (10),

$$\rho V_L^2 = 2.982 \text{ gr/cm} \cdot \text{sec}^2 \rightarrow V_L$$
$$= 0.9133 \times 10^6 \text{ cm/sec} \qquad (11)$$

Comparing (11) with (7), $\varDelta V = 0.002 \times 10^6$ cm/sec. Therefore, $\varDelta \rho V_L^2 = 0.013$. This much should be higher in C_{11}. $C_{11} = 2.985$ in Mbar (This is equal to 298.5 GPa).
And, $2 \rho V_T^2 = 3.1036$ from the '-' case in equation (5) with (8) with similar procedure,

$$\varDelta \rho V_T^2 = - 0.004, \ \rho V_T^2 = 1.5518 \text{ in Mbar}$$
$$\text{(i.e., 155.2 GPa)} \qquad (12)$$

From [110] plane measurements, of which plane (110) is parallel perfectly, and thickness of 0.2405 inch, we can get the following results :

$$\rho V_L^2 = 3.527 \text{ x } 10^{12} = C_{11} + C_{44} - C'$$
$$- \rho V_{T2}^2 = 1.0098 \text{ x } 10^{12} = C' \qquad (13)$$
$$- \rho V_{T1}^2 = 1.5618 \text{ x } 10^{12} = C_{44}$$

From (13),

$$C_{11} = 297.5 \text{ GPa}, \ C_{44} = 156.2 \text{ GPa},$$
$$C' = 101.0 \text{ GPa}, \ C_{12} = C_{11}\text{-}2C' = 95.5 \text{ GPa} \qquad (14)$$

Velocity measurement data for (110) plane by both longitudinal and transverse waves are not given, because of the similarity to the (100) plane measurement.

The bulk moduli of MgO can be calculated using the relation of $K_S = (C_{11} + 2C_{12})/3$ for (100) and (110) planes to be 163.2 GPa and 162.6 GPa, respectively.